

## Indium tin oxide thin films for organic light-emitting devices

H. Kim,<sup>a)</sup> A. Piqué, J. S. Horwitz, H. Mattoussi, H. Murata, Z. H. Kafafi,  
and D. B. Chrisey

Naval Research Laboratory, Washington DC 20375

(Received 15 February 1999; accepted for publication 9 April 1999)

High-quality indium tin oxide (ITO) thin films (150–200 nm) were grown on glass substrates by pulsed laser deposition (PLD) without postdeposition annealing. The electrical, optical, and structural properties of these films were investigated as a function of substrate temperature, oxygen pressure, and film thickness. PLD provides very uniform ITO films with high transparency ( $\geq 85\%$  in 400–700 nm spectrum) and low electrical resistivity ( $2\text{--}4 \times 10^{-4} \Omega \text{ cm}$ ). The Hall mobility and carrier density for a 170-nm-thick film deposited at 300 °C are  $29 \text{ cm}^2/\text{V s}$  and  $1.45 \times 10^{21} \text{ cm}^{-3}$ , respectively. Atomic force microscopy measurements of the ITO films indicated that their root-mean-square surface roughness ( $\sim 5 \text{ \AA}$ ) is superior to that ( $\sim 40 \text{ \AA}$ ) of commercially available ITO films deposited by sputtering. ITO films grown at room temperature by PLD were used to study the electroluminescence (EL) performance of organic light-emitting devices. The EL performance was comparable to that measured with commercial ITO anodes. © 1999 American Institute of Physics. [S0003-6951(99)00123-0]

Indium tin oxide (ITO) thin films have been studied extensively for optoelectronic device applications because of their unique transparent and conducting properties. ITO is a highly degenerate *n*-type semiconductor, that has low electrical resistivity of  $2\text{--}4 \times 10^{-4} \Omega \text{ cm}$ . ITO is a wide band gap (3.3–4.3 eV) material which shows high transmission in the visible and near-IR regions of the spectrum. ITO has been used in a wide range of applications such as liquid crystal flat panel display and solar cell devices.<sup>1</sup> Because ITO films have shown good efficiency for hole injection into organic materials, they have also been widely utilized as the anode contact for organic light-emitting diodes (OLEDs).<sup>2</sup> Several deposition techniques have been used to grow ITO thin films including chemical vapor deposition,<sup>3</sup> magnetron sputtering,<sup>4,5</sup> evaporation,<sup>6</sup> spray pyrolysis,<sup>7</sup> and pulsed laser deposition (PLD).<sup>8,9</sup> In this letter, we report a study of the electrical, optical, and structural properties of ITO films grown on glass substrates by PLD and the performance characteristics of OLEDs using PLD ITO anodes.

Films were deposited using a KrF excimer laser [Lambda Physics LPX 305, 248 nm and 30 ns full-width at half-maximum (FWHM)]. The laser was operated at 10 Hz and focused through a 50 cm focal length lens onto a rotating target at a 45° angle of incidence. The energy density of laser beam at the target surface was maintained at  $2 \text{ J/cm}^2$ . The target-substrate distance was 4.7 cm. Before deposition, the target was ablated with a laser fluence of  $2 \text{ J/cm}^2$  for 5000 shots. The geometry of this PLD system produced uniform films over  $1.5 \times 1.5 \text{ cm}^2$  substrate areas with a thickness variation of less than 10%. The substrate was attached with a stainless steel mask to a substrate holder, which was heated by two quartz lamps. The substrate temperature was held constant during deposition using a temperature controller

with input from a thermocouple imbedded in the center of the stainless steel substrate holder.

The target was a 2 in. diameter by 0.25-in.-thick sintered disk containing  $\text{In}_2\text{O}_3$  (95%)+ $\text{SnO}_2$  (5%) by weight. The substrates were cleaned in an ultrasonic cleaner for 10 min with acetone and then methanol. After evacuating the chamber to a pressure of  $10^{-6}$  Torr, the substrates were heated to the desired temperature in the desired oxygen pressure. During the deposition, the oxygen pressure in the chamber ranged from 1 to 100 mTorr. After deposition, films were slow cooled to room temperature at the same oxygen pressure.

The film thickness was measured by a stylus profilometer. The sheet resistance measurements were performed using a four-point probe. The deposition rate decreased from 0.85 to  $0.39 \text{ \AA/pulse}$  with increasing oxygen pressure from 1 to 100 mTorr. The oxygen pressure also affected the thickness uniformity of the films; as the oxygen pressure decreased from 100 to 10 mTorr, the thickness uniformity improved.

The sheet resistance and resistivity were calculated from the average of three measurements for each film. Hall mobility and carrier density measurements were made using the Van der Pauw method at room temperature with a field strength of 5 kG. Optical transmission measurements were made using an UV-visible-near IR spectrophotometer. The structure and surface morphology of the films were determined using x-ray diffraction (XRD) ( $\text{Cu } K\alpha$ ,  $\lambda = 1.5406 \text{ \AA}$ ), scanning electron microscopy (SEM), and atomic force microscopy (AFM).

Figure 1 shows the dependence of the electrical resistivity on oxygen pressure for ITO films grown at different substrate temperatures. At low substrate deposition temperatures, the resistivity of the film is very sensitive to oxygen pressure. Low resistivity values were observed in a narrow pressure range (10–15 mTorr). As the substrate deposition temperature increased, the resistivity of the ITO films became less dependent on the oxygen pressure. The oxygen

<sup>a)</sup>Institute for Materials Science, School of Engineering and Applied Science, George Washington University, Washington DC 20052; Electronic mail: hskim@ccf.nrl.navy.mil

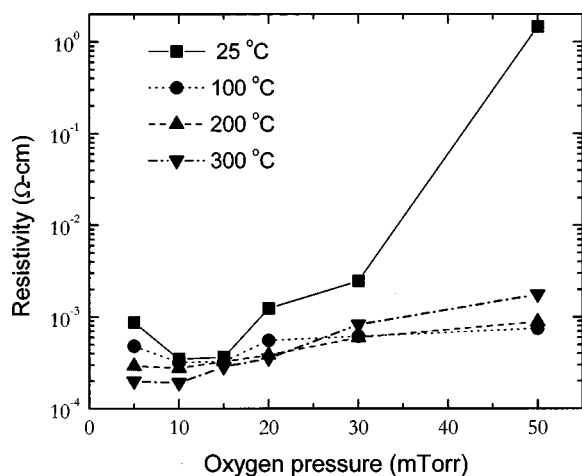


FIG. 1. Electrical resistivity ( $\rho$ ) of the ITO films, plotted as a function of oxygen pressure at different substrate deposition temperatures.

pressure dependence of the resistivity of the films (grown at low temperatures) can be explained by the number of oxygen vacancies in the film. Oxygen vacancies generate free carriers. An increase in the number of oxygen vacancies leads to an increase in conductivity. Hence, the resistivity of the ITO films decreases with decreasing oxygen pressure from 50 to 10 mTorr due to an increase in the number of oxygen vacancies. However, the resistivity of the ITO films increases with a further decrease in the oxygen pressure ( $<10$  mTorr). The resistivity values of the ITO films grown in pressure of  $10^{-5}$  Torr (without oxygen addition) at 25 and 300 °C were 0.69 and  $7.6 \times 10^{-4} \Omega \text{ cm}$ , respectively. A severe oxygen deficiency may cause lattice structural disorder and reduce the mobility of carriers.<sup>10</sup>

The substrate deposition temperature affects the electrical properties of the ITO films (Table I). The resistivity of the ITO films decreased from  $3.8 \times 10^{-4}$  to  $1.9 \times 10^{-4} \Omega \text{ cm}$  as the substrate temperature was increased from 25 to 300 °C. The decrease in resistivity can be explained by the fact that the crystalline size (Table I) increases significantly with increasing the substrate temperature, thus reducing the grain boundary scattering and increasing the conductivity. This decrease in resistivity can also be correlated with the observed increase in carrier mobility.

The substrate deposition temperature also affects the optical properties of the present ITO films (Table I). The average % transmission in the visible range of the optical spectrum increased from 85% to 92% as the substrate deposition

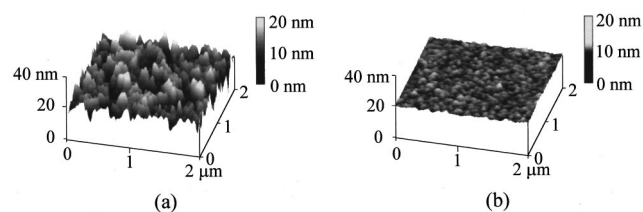


FIG. 2. AFM images ( $2 \mu\text{m} \times 2 \mu\text{m}$ ) of the ITO films grown on glass substrates by (a) sputtering (supplied by Planar America) and (b) PLD. Note that the scale in the  $z$  direction (20 nm/div.) is greatly expanded with respect to the scales in the  $x$  and  $y$  directions ( $\mu\text{m}/\text{div.}$ ) and therefore, in fact, the crystallites are flat and broad in the lateral direction.

temperature was increased from 25 to 300 °C. The optical properties of the ITO films were also affected by oxygen pressure and film thickness. We found that the optical transmission increased as the oxygen pressure was increased from 10 to 50 mTorr for the thicker ( $>300$  nm) films deposited at various temperatures (25–300 °C). All of films grown in pressure of  $10^{-5}$  Torr (without oxygen addition) showed poor optical transmission ( $<50\%$ ). The band gap,  $E_g$ , was also affected by substrate deposition temperature. The band gap increased from 3.90 to 4.21 eV as the substrate temperature was increased from 25 to 300 °C. This increase in band gap may be attributed to the increased carrier concentration,  $N$ , as shown Table I. The increase in band gap can be explained by the Burstein–Moss shift:  $E_g \propto N^{2/3}$ .<sup>11</sup>

ITO films deposited at room temperature (RT) were completely amorphous as determined by x-ray diffraction. Despite their completely amorphous structure, the resistivity of the RT films was observed to be fairly low ( $\sim 3.8 \times 10^{-4} \Omega \text{ cm}$ ). Films deposited at higher temperatures ( $>100$  °C) had a polycrystalline cubic structure with a lattice parameter of 10.22–10.31 Å which is larger than the Joint Committee on Powder Diffraction Standards (JCPDS)<sup>12</sup> value of 10.118 Å for the  $\text{In}_2\text{O}_3$  powder. The increase in lattice parameter of the ITO films over bulk materials can be explained by the substitutional incorporation of  $\text{Sn}^{4+}$  ions into  $\text{In}^{3+}$  sites and/or the incorporation of Sn ions in the interstitial positions. For the films deposited at 300 °C, the intensity of the (222) reflection indicated that this was a preferred orientation of the films. The (221), (400), (422), and (622) reflections were observed to be minor peaks.

Since the organic thin films employed in OLEDs are directly deposited on the ITO anode, the surface properties of the ITO may affect the characteristics of the device. Figure 2

TABLE I. Electrical and optical properties of ITO films deposited at different temperatures. The variations of sheet resistance and resistivity were due to thickness variation of the films. All transmission values were normalized by the transmission of a bare glass substrate. The values of energy gap,  $E_g$ , were determined by extrapolations of the straight regions of the plots of square of the absorption coefficient  $\alpha^2$  vs photon energy  $h\nu$ . The absorption coefficient  $\alpha$  was determined by the equation,  $\alpha = \ln(1/T)/d$ , where  $T$  is transmission and  $d$  is film thickness. Grain sizes were calculated using the Scherrer formula for the (222) reflection of the films.

Growth temperature (°C)	Grain size (nm)	Sheet resistance ( $\Omega/\text{sq.}$ )	Resistivity ( $10^{-4} \Omega \text{ cm}$ )	Carrier density ( $10^{20} \text{ cm}^{-3}$ )	Mobility ( $\text{cm}^2 \text{ V}^{-1} \text{ s}^{-1}$ )	Energy gap $E_g$ (eV)	Mean transmission (%)
25	--	$28.1 \pm 0.82$	$3.8 \pm 0.43$	8.5	12.8	3.90	85
100	8	$18.2 \pm 0.40$	$2.9 \pm 0.23$	10.0	16.8	4.08	88
200	14	$12.9 \pm 0.42$	$2.1 \pm 0.17$	13.2	27.3	4.15	90
300	20	$11.2 \pm 0.75$	$1.9 \pm 0.18$	14.5	29.4	4.21	92

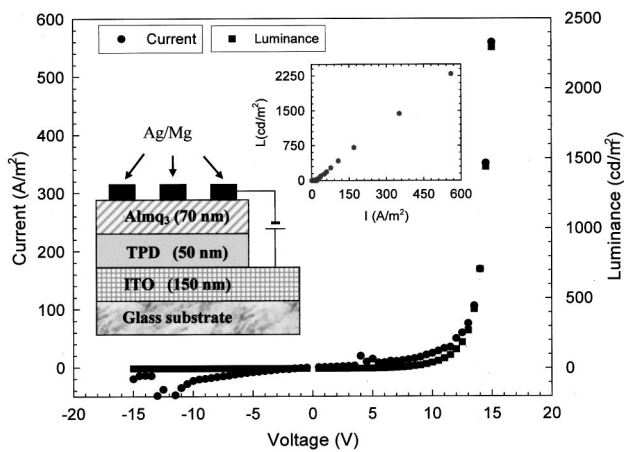


FIG. 3. Current-voltage-luminance ( $I$ - $V$ - $L$ ) characteristics of a heterostructure device schematically represented in the insert. ITO film, grown at room temperature in oxygen pressure of 10 mTorr, was used in this device.

shows two AFM images ( $2\ \mu\text{m} \times 2\ \mu\text{m}$ ) of ITO films deposited by sputtering (supplied by Planar America) and PLD. Prior to AFM measurements, the films were washed with methanol and blown dry with nitrogen gas. The root-mean-square (rms) surface roughness for the ITO films deposited by PLD at a substrate temperature of  $300\ ^\circ\text{C}$  and oxygen pressure of 10 mTorr is  $\sim 4.4\ \text{\AA}$  compared to a value of  $\sim 12.5\ \text{\AA}$  for the bare glass substrate. However, the rms of the film deposited by sputtering is  $\sim 39\ \text{\AA}$  compared to a value of  $16.2\ \text{\AA}$  for the bare glass substrate. This indicates that the present PLD ITO films show lower surface roughness than that of sputtered ITO films. Even though the surface of the PLD ITO films was very smooth as indicated by AFM measurements, other surface features ( $0.1$ – $1\ \mu\text{m}$ ) were observed in the deposited films. The average feature size depended on the deposition temperature and oxygen background gas pressure. The average feature size decreased with increasing deposition temperature from 25 to  $300\ ^\circ\text{C}$  and decreasing oxygen pressure from 100 to 10 mTorr. Particulates in the deposited film could cause a cathode-to-anode short circuit. However, no leakage of current was observed in OLEDs with the observed features.

Figure 3 shows current-voltage-luminance output ( $I$ - $V$ - $L$ ) characteristics of OLEDs with the ITO anode grown at room temperature by PLD. The device structure used in this study is made of a hole transport layer (HTL,  $\sim 500\ \text{\AA}$ ) of  $N$ ,  $N'$ -diphenyl- $N$ ,  $N$ -bis(3-methylphenyl)1,1'-diphenyl-4,4'-diamine (TPD), and an electron transport/emitting layer (ETL/EML,  $\sim 700\ \text{\AA}$ ) of tris(4-methyl-8-hydroxyquinolinolato) aluminum (III) ( $\text{Almq}_3$ ). The cathode contact deposited on top of the ETL is an alloy of Mg:Ag (ratio=12:1 and a thickness of  $1000\ \text{\AA}$ ). Details of fabrication are described elsewhere.<sup>13–15</sup> The active area of the device is  $\sim 2 \times 2\ \text{mm}^2$ . The current-voltage-luminance ( $I$ - $V$ - $L$ ) data were taken (in  $\text{N}_2$  atmosphere) using a Keithley current/voltage source and a luminance meter (Minolta

LS-110). The  $I$ - $V$  and  $L$ - $V$  curves show a typical diode behavior, with current and power output observed only in the forward bias. Furthermore, the data for  $I$  and  $L$  superimpose quite well, in agreement with what is reported with commercial ITO. The device external quantum efficiency measured for such a heterostructure device was  $\eta_{\text{ext}} \cong 1.3\%$ . This value is comparable to those reported recently ( $\eta_{\text{ext}} \cong 1.5\%$ – $2.5\%$ ) using commercial ITO from different sources as the anode contact.<sup>13–15</sup> The above value for  $\eta_{\text{ext}}$  indicates that ITO films, grown by PLD at RT, are of good quality and could have a potential for a dramatic increase in OLED external quantum efficiency.

In conclusion, high-quality ITO films have been grown on glass substrates by PLD without a postdeposition anneal. For a 170-nm-thick films deposited at  $300\ ^\circ\text{C}$  in the same oxygen pressure, the resistivity is  $1.9 \times 10^{-4}\ \Omega\ \text{cm}$  and the average % transmission in the visible range is  $\sim 92\%$ . These values are similar to those measured ( $1.95 \times 10^{-4}\ \Omega\ \text{cm}$  and 90%) from commercial ITO films (grown by sputtering). PLD ITO films show lower surface roughness than commercial ITO films, with a substantially smaller surface roughness (by  $\sim 1$  order of magnitude). We used these ITO films as the anode contact in OLEDs and studied the device performance. EL efficiencies comparable to those reported with commercial ITO have been measured for heterostructure devices made of TPD/ $\text{Almq}_3$ . This indicates the promise of the present approach for making good quality ITO films with a potential application in OLEDs.

$\text{Almq}_3$  was kindly supplied by Professor Junji Kido of Yamagata University, Japan. This work was financially supported by Office of Naval Research. We would like to thank Dr. Eric Jackson for his help relating Hall effect measurements. The authors thank Dominic Rumbola and Melissa Strausberg for their assistance.

- <sup>1</sup>H. L. Hartnagel, A. L. Dawar, A. K. Jain, and C. Jagadish, *Semiconducting Transparent Thin Films* (Institute of Physics, Bristol, 1995).
- <sup>2</sup>C. W. Tang and S. A. Van Slyke, *Appl. Phys. Lett.* **51**, 913 (1987).
- <sup>3</sup>T. Maruyama and K. Fukui, *Thin Solid Films* **203**, 297 (1991).
- <sup>4</sup>W.-F. Wu, B.-S. Chiou, and S.-T. Hsieh, *Semicond. Sci. Technol.* **9**, 1242 (1994).
- <sup>5</sup>M. Buchanan, J. B. Webb, and D. F. Williams, *Appl. Phys. Lett.* **37**, 213 (1980).
- <sup>6</sup>P. Nath, R. F. Bunshah, B. M. Basol, and O. M. Staffsud, *Thin Solid Films* **72**, 463 (1980).
- <sup>7</sup>V. Vasu and A. Subrahmanyam, *Thin Solid Films* **193/194**, 696 (1990).
- <sup>8</sup>J. P. Zheng and H. S. Kwok, *Appl. Phys. Lett.* **63**, 1 (1993).
- <sup>9</sup>C. Coutal, A. Azema, and J.-C. Roustau, *Thin Solid Films* **288**, 248 (1996).
- <sup>10</sup>T. Karasawa and Y. Miyata, *Thin Solid Films* **233**, 135 (1993).
- <sup>11</sup>E. Burstein, *Phys. Rev.* **93**, 632 (1954); T. S. Moss, *Proc. Phys. Soc. London, Sect. B* **67**, 775 (1964).
- <sup>12</sup>JCPDS Card No. 06-0416.
- <sup>13</sup>J. Kido and Y. Iizumi, *Chem. Lett.* (10), 963 (1997).
- <sup>14</sup>J. Kido and Y. Iizumi, *Appl. Phys. Lett.* **73**, 2721 (1998).
- <sup>15</sup>H. Murata, C. D. Merritt, H. Mattoussi, and Z. H. Kafafi, *Proc. SPIE* **3476**, 88 (1998).